Geochemical Perspectives Letters

Dissecting the complex Ne-Ar-N signature of asteroid Ryugu by step-heating analysis

J. Gamblin, E. Füri, B. Marty, L. Zimmermann, D.V. Bekaert

Supplementary Information

The Supplementary Information includes:

- Detailed Methodology
- Figures S-1 and S-2
- Tables S-1 and S-2
- Supplementary Information References

Detailed Methodology

Ryugu sample C0015

Sample C0015 (Fig. S-1) is a single particle (1.8 ± 0.2 mg; weighed at JAXA's curation facility) that was collected during the second touchdown of JAXA's Hayabusa2 spacecraft on asteroid (162173) Ryugu and corresponds to surface or sub-surface material. It was kept under ultra-pure N_2 during weighing, storage, and shipping in a stainless-steel capsule to avoid contamination by Earth's atmosphere. At the Centre de Recherches Pétrographiques et Géochimiques (CRPG) noble gas facility, the particle was placed into a ZnSe-windowed laser chamber within a N_2-filled glove box. The isotopic composition of N_2 used for sample handling at CRPG was close to atmospheric. The sample pits were covered by a second ZnSe window to prevent the particle from bouncing out of position during laser heating and degassing. Once the chamber was connected to the purification line of the Noblesse–HR (3F4M) noble gas mass spectrometer, it was pumped to ultra-high vacuum (~10^{-9} bar) using a turbomolecular pump and baked at 100 °C overnight to remove any adsorbed terrestrial gases from the inner surfaces of the laser chamber and any adsorbed dry N_2 from the particle surface.

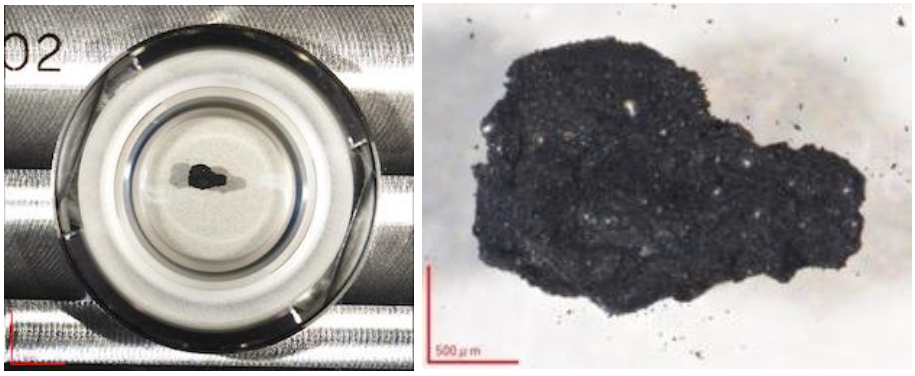

Figure S-1 Optical microscope images of particle C0015 in its sample storage dish taken at JAXA's curation facility (images from Hayabusa2, Ryugu Sample Curatorial Dataset, Institute of Space and Astronautical Science (ISAS), Japan Aerospace Exploration Agency (JAXA): https://doi.org/10.17597/ISAS.DARTS/CUR-Ryugu-description).

Step-heating gas extraction

Noble gases (Ne, Ar) and N were extracted under static vacuum from particle C0015 by step-heating using a 10.6 µm CO_2-laser (MIR10[2], Elemental Scientific) at increasing power (*i.e.* 1 to 45 % of the total power of 32 W). A total of 85 heating steps were performed, allowing the successive release of gases contained in different carrier phases. When a large amount of gas was extracted at a given laser power, further extraction steps were performed at the same power until the amount of extracted gases decreased. A high-resolution CCD video camera above the extraction chamber permitted to monitor sample heating (Fig. S-2) and melting, which was achieved at 24 % of the maximum laser power. A limitation of this method is the lack of knowledge of the heating temperature of the sample. In addition, during the extractions at high temperature, vapour deposits began to accumulate on the second window covering the sample, thus reducing the heating efficiency and the visibility of the sample. Gentle tapping against the laser chamber permitted to move the window to a clean spot. Notably, after steps #70 and #71 (at 17 % of the maximum laser power), for which the N isotope ratio was significantly lower than for the previous steps (Fig. 1c), the window was moved and the laser power lowered to 9 % to ensure that the laser beam still went through the window without loss by absorption. For the first 26 steps, the particle was heated for 4 min, whereas for the following 59 steps, the heating duration was increased to 12 min.

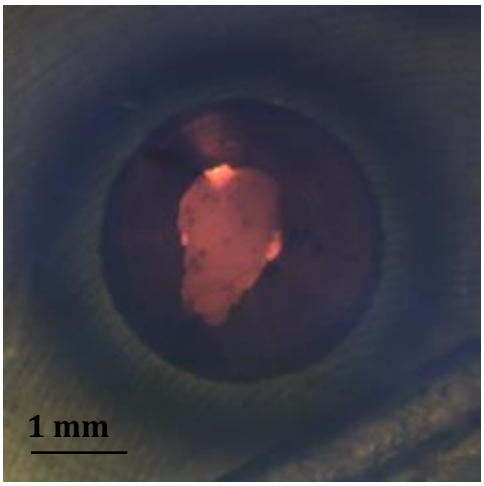

Figure S-2 Camera view of particle C0015 at heating step #73 and 15 % of the maximum laser power.

Gas purification

Following gas extraction, the gas was split into two calibrated volumes for specific noble gas (Ne, Ar) and N purifications (Zimmermann *et al.*, 2009).

Within the all-metal line used for noble gas purification, Ar was first separated from Ne by adsorption onto a charcoal finger held at –196 °C using liquid nitrogen for 5 min. Neon was then purified by exposure to a Ti-sponge getter held at 600 °C for 10 min, followed by exposure to a second charcoal finger at liquid nitrogen temperature and two SAES Ti-Al getters at room temperature for 10 min. After Ne inlet into the Noblesse–HR noble gas mass spectrometer, two GP-50 SAES getters at room temperature, connected to the source and detector blocks, and an additional charcoal finger held at –196 °C were used for 10 min prior to the start of the analysis and during the entire analytical sequence to minimise contributions of $^{40}Ar^{2+}$, H_2O^+, HF^+, and $^{44}CO_2^{2+}$ to the $^{20,22}Ne^+$ signals and preserve a constant H_2 level.

Following the Ne analysis, Ar was desorbed from the charcoal finger and purified by exposure to the Ti-sponge getter at 600 °C and the two SAES getters at room temperature for 10 min. During the Ar analysis, the two GP-50 SAES getters were used to minimise the $H^{35,37}Cl^+$ signals and maintain a constant, low H_2 level.

In parallel, N was purified within a Pyrex and quartz-glass line based on the procedure previously described by Humbert *et al*. (2000), Hashizume and Marty (2004), and Zimmermann *et al.* (2009). Nitrogen (and other species such as H, C, S) was oxidised thanks to the O_2 released during heating of CuO sticks from 450 °C to 900 °C for 25 min. A U-shaped cold trap at –180 °C trapped the different oxidised species except for NO_X. The CuO sticks were then gradually cooled to 800 °C, 700 °C, 600 °C, 500 °C, and 300 °C (15 min for each step) to re-absorb excess O_2 (Robinson and Kusakabe, 1975) and reduce NO_X to molecular nitrogen (N_2). Once the CuO sticks reached 600 °C, a glass finger containing several platinum foils was cooled to –175 °C to improve the trapping efficiency of the remaining oxidised impurities. Prior to expanding N_2 into the Noblesse–HR noble gas mass spectrometer, the pressure was monitored using a hot cathode ion gauge to ensure that an appropriate amount of gas was inlet to match the $^{28}N_2^+$ signal of air standard measurements and to avoid saturation of the detectors. If required, only a fraction of the extracted and purified N_2 was inlet and analysed.

Noble gas mass spectrometry analyses

Purified gases (Ne, Ar, N_2) were analysed sequentially using a Noblesse–HR noble gas mass spectrometer (Nu Instruments) at a trap current of 150 µA and specific source settings to maximise sensitivity and minimise instrumental mass fractionation for each gas species. The three isotopes of Ne were measured simultaneously on three ion counters ($^{22}Ne^+$ on IC0, $^{21}Ne^+$ on IC2, $^{20}Ne^+$ on IC3) for 25 cycles. The $^{40}Ar^{++}$ signal was monitored during each cycle; however, given that the $^{40}Ar^{++}$ peak is partially resolved from that of $^{20}Ne^+$, no correction was applied to the $^{20}Ne^+$ signal. The $^{44}CO_2^+$ signal was also measured during each cycle by peak-jumping, and the $^{22}Ne^+$ signal was corrected using a $^{44}CO_2^{++}/^{44}CO_2^+$ ionisation ratio of 1.2 %. (The $^{44}CO_2^{++}/^{44}CO_2^+$ ionisation ratio was previously determined from background CO_2 in the mass spectrometer, and by varying the CO_2 pressure by partially closing the valve to the source getter). The $^{21}Ne^+$ signal was measured at the peak center; no hydride ($^{20}NeH^+$) correction was performed because the getter allowed maintaining a low H_2 background. After releasing Ar from the charcoal finger, the three Ar isotopes were analysed in multi-collection mode ($^{40}Ar^+$ on Fa0 with a 10^{11} Ω resistor, $^{38}Ar^+$ on IC2, $^{36}Ar^+$ on IC3) for 25 cycles. The three isotopologues of N_2 were also analysed simultaneously at mass 28 ($^{14}N^{14}N^+$) on Fa2 with a 10^{11} Ω resistor, mass 29 ($^{14}N^{15}N^+$) on Fa1 with a 10^{12} Ω resistor, and mass 30 ($^{15}N^{15}N^+$) on IC0, after measuring the $^{12,13}C^{16}O^+$ signals by changing the voltage of the LIN2 lense. Following data acquisition, which comprised 25 measurement cycles, the $^{14}N^{14}N^+$ and $^{14}N^{15}N^+$ signals were obtained by correcting for the $^{12}C^{16}O^+$ and $^{13}C^{16}O^+$ contributions, respectively.

Measured ion signals were processed using the "Nu Instruments Calculation Editor" (NICE); detector baselines and contributions from interfering species were subtracted from the signals of interest, and isotope ratios were calculated for each measurement cycle. The "Nu Noble" software was then used to extrapolate the corrected ion signals and isotope ratios to $t = 0$ using a linear (for Ne and Ar) or exponential equation (for N_2). Baseline- and interference-corrected Ne, Ar, and N_2 ion signals, as well as $^{20}Ne/^{22}Ne$, $^{21}Ne/^{22}Ne$, $^{40}Ar/^{36}Ar$, $^{38}Ar/^{36}Ar$, $^{28}N_2/^{29}N_2$, and $^{29}N_2/^{30}N_2$ ratios, extrapolated to $t = 0$, are available for download at https://doi.org/10.24396/ORDAR-144.

To determine the analytical sensitivity and the instrumental mass fractionation of the Noblesse–HR noble gas mass spectrometer, purified air standard aliquots were analysed at least twice a week for Ne, Ar, and N_2. The reproducibility of air standard measurements was 2.1 % for ^{20}Ne, 1.5 % for ^{36}Ar, and 4.5 % for $^{28}N_2$ abundances, and 0.59 % for $^{20}Ne/^{22}Ne$, 1.77 % for $^{21}Ne/^{22}Ne$, 0.20 % for $^{38}Ar/^{36}Ar$, and 0.07% for $^{28}N_2/^{29}N_2$ isotope ratios over the 20-week measurement period. Noble gas (Ne, Ar) and N_2 abundances were calculated based on the sensitivity of the mass spectrometer using equation S-1 (Zimmermann and Bekaert, 2020):

$$n = \frac{U \times V_I}{R \times S \times d \times 760 \times V_M} \quad \text{Eq. S-1,}$$

where n is the abundance (mol), U is the ion signal (V), V_I is the volume of the laser chamber (24.35 cm^3), R is the resistance at the collector outlet (10^{11} or 10^{12} Ω), S is the sensitivity ($4.9 \pm 0.1 \times 10^{-5}$ A/Torr for ^{20}Ne, $2.26 \pm 0.03 \times 10^{-4}$ A/Torr for ^{36}Ar, and $1.30 \pm 0.06 \times 10^{-4}$ A/Torr for $^{28}N_2$, on average), d is the dilution coefficient, and V_M is the molar volume (22,414 cm^3/mol). Procedural blanks (laser off) for a 4 min-long extraction were $1.8 \pm 0.2 \times 10^{-16}$ mol ^{20}Ne, $1.2 \pm 0.1 \times 10^{-17}$ mol ^{36}Ar, and $4.5 \pm 1.4 \times 10^{-12}$ mol $^{28}N_2$, and $3.3 \pm 0.3 \times 10^{-16}$ mol ^{20}Ne, $1.4 \pm 0.2 \times 10^{-17}$ mol ^{36}Ar, and $3.8 \pm 1.3 \times 10^{-12}$ mol $^{28}N_2$ for a 12 min-long extraction.

Blank-corrected Ne, Ar, and N_2 abundances (in mol), and $^{20}Ne/^{22}Ne$, $^{21}Ne/^{22}Ne$, $^{38}Ar/^{36}Ar$, and $\delta^{15}N$ values corrected for instrumental mass fractionation, for the 85 extraction steps of particle C0015, as well as calculated bulk abundances and isotope ratios, are available for download at https://doi.org/10.24396/ORDAR-144. Uncertainties of blank-corrected Ne, Ar, and N_2 abundances and isotopic ratios were calculated using the Monte Carlo method. Isotope ratios of heating-steps with ≥30 % blank contributions are excluded from the figures and further discussions. Nitrogen isotope ratios are given in the $\delta^{15}N$ notation:

$$\delta^{15}N\ (‰) = \left(\frac{1 + 2 \times (^{28}N_2/^{29}N_2)_{atm}}{1 + 2 \times (^{28}N_2/^{29}N_2)_{measured}} - 1\right) \times 1000 \quad \text{Eq. S-2,}$$

where $(^{28}N_2/^{29}N_2)_{atm}$ is the isotopic composition of atmospheric N_2 (136.05; Nier, 1950).

Table S-1 Calculated bulk Ne-Ar-N concentrations and isotope ratios of Ryugu particle C0015. Uncertainties on the abundance-weighted average values (1σ) were calculated using a Monte Carlo method. Uncertainties of noble gas and N concentrations are mainly controlled by the uncertainty on the sample mass.

^{20}Ne (mol/g)	$^{20}Ne/^{22}Ne$	^{36}Ar (mol/g)	$^{38}Ar/^{36}Ar$	N (ppm)	$\delta^{15}N$ (‰)
$2.13 \pm 0.23 \times 10^{-9}$	13.07 ± 0.02	$1.80 \pm 0.20 \times 10^{-10}$	0.1865 ± 0.0001	1760 ± 195	+24.43 ± 0.17

Nitrogen components in CI chondrites and Ryugu

Several previous studies have attempted to dissect the different N components and their isotopic compositions in CI chondrites and Ryugu samples. High-resolution stepped combustion analyses of Orgueil chips revealed that most of the N in CIs is released at temperatures between 400 ˚C and 600 ˚C due to the combustion of organic matter (*e.g.*, Grady *et*

al., 2002; Sephton *et al*., 2003). Nanodiamonds also contribute to the N release within this temperature range, whereas graphite and silicon carbides have higher combustion temperatures of 500 to 700 ˚C and 1200 to 1600 ˚C, respectively (Sephton *et al*., 2003, and references therein). The heterogeneous distribution of N-bearing components in carbonaceous chondrites (*e.g*., Kerridge, 1985) and Ryugu samples (Nakamura *et al*., 2022) has also been highlighted. Notably, ^{15}N-hotspots (δ^{15}N up to +3000 ‰) and ^{15}N-coldspots (δ^{15}N down to –150 ‰), identified by *in situ* secondary ion mass spectrometry analyses, were inferred to control the bulk δ^{15}N variations detected in Ryugu particles by the Phase-2 curation team (Institute for Planetary Materials, Okayama University; Nakamura *et al*., 2022).

The predominant N-bearing phase in CIs is insoluble organic matter (IOM) (Matsumoto *et al*., 2024), which has a δ^{15}N value of about +31 ‰ (Alexander *et al*., 2007). Given that IOM is sensitive to brief thermal events such as solar heating and impacts (Quirico *et al*., 2018), the N signature of this component may have been modified by regolith processes at Ryugu's surface. Nonetheless, the N isotope ratios of insoluble carbonaceous residues of Ryugu are close to the IOM value (+17.4 ± 1. 9 ‰ and +30 ± 4.3 ‰ in two different samples; Yabuta *et al*., 2023). Other N-bearing phases can show highly variable δ^{15}N values. For example, the δ^{15}N values of C-rich exogenous clasts in Ryugu samples vary from –505 ± 149 ‰ to +3219 ± 672 ‰ (Nguyen *et al*., 2023). Furthermore, Barosch *et al*. (2022) and Nguyen *et al*. (2023) identified various types of presolar grains in Ryugu material, such as presolar oxides, silicates, silicon carbide (SiC), graphite, and C-anomalous organics, which are known to show a wide range of δ^{15}N values inherited from their different stellar sources (*e.g*., –825 ± 189 ‰ to +705 ± 428 ‰ for SiC and–536 ± 465 ‰ to +1512 ± 221 ‰ for presolar graphite and SiC; Nguyen *et al*., 2023). The N isotopic composition of presolar nanodiamonds, the carrier phase of Ne-HL, could not be determined in Ryugu samples due to their small size (Barosch *et al*., 2022); however, previous measurements in primitive chondrites revealed that they contain abundant N with strikingly negative δ^{15}N values down to –348 ± 7 ‰ (Russell *et al*., 1996). It is noteworthy that the isotopic composition of N in phase Q is poorly known due to impossibility of isolating pure Q; based on stepped combustion analyses of carbonaceous chondrites, Verchovsky (2017) argued that phase Q carries isotopically light N with a δ^{15}N value <–150 ‰ and possibly similar to the solar value (*i.e*. $\delta^{15}N_{Sun}$ = –383 ± 8 ‰; Marty *et al*., 2011) (Verchovsky, 2017). All of the aforementioned N-bearing phases (*i.e*. organics, various presolar phases, phase Q) – as well as nitrides (Matsumoto *et al*., 2024) and NH-rich compounds (Pilorget *et al*., 2022) – are likely present in Ryugu particle C0015 and contribute to the δ^{15}N variations observed during step-heating analysis.

Table S-2 Nitrogen abundance and isotopic composition (δ^{15}N) of CI chondrites and Ryugu samples.

Sample	N (ppm)	δ^{15}N (‰)	Reference
Alais (CI1)	1250	+31	Kerridge (1985)
	1900	+45.7	Pearson *et al.* (2006)
	1800	+41.8	Pearson *et al.* (2006)
	2400	+61.1	Pearson *et al.* (2006)
	2100	+56.5	Pearson *et al.* (2006)
	1800	+54.7	Pearson *et al.* (2006)
Ivuna (CI1)	1855	+52	Kerridge (1985)
	2070	+44.9	Alexander *et al.* (2012)
	1113.42 ± 36.26	+36.4 ± 0.4	Hashizume *et al.* (2024)
Orgueil (CI1)	1476	+46.2	Injerd and Kaplan (1974)
	1360	+39	Robert and Epstein (1982)
	1999.6	+32	Grady *et al.* (2002)
	2070	+32.2	Sephton *et al.* (2003)
	5600	+38.0	Pearson *et al.* (2006)
	8200	+41.4	Pearson *et al.* (2006)
	2100	+54.2	Pearson *et al.* (2006)
	1490	+44.1	Alexander *et al.* (2012)
	2080	+35.9	Alexander *et al.* (2012)

Y-980115 (CI1 or CY)	900 438	–2.8 +4.0 ± 0.3	Chan *et al.* (2016) Hashizume *et al.* (2024)
Ryugu A0022	1170	+40.53	Nakamura *et al.* (2022)
Ryugu A0033	1660	+17.82	Nakamura *et al.* (2022)
Ryugu A0035	1930	+52.08	Nakamura *et al.* (2022)
Ryugu A0048	1290	+35.00	Nakamura *et al.* (2022)
Ryugu A0073	1930	+52.34	Nakamura *et al.* (2022)
Ryugu A0078	1810	+50.94	Nakamura *et al.* (2022)
Ryugu C0008	1590	+46.23	Nakamura *et al.* (2022)
Ryugu C0019	1010	+26.80	Nakamura *et al.* (2022)
Ryugu C0027	1030	+22.66	Nakamura *et al.* (2022)
Ryugu C0079	1070	+22.85	Nakamura *et al.* (2022)
Ryugu C0081	2160	+53.01	Nakamura *et al.* (2022)
Ryugu C0082	1910	+0.37	Nakamura *et al.* (2022)
Ryugu A0106 #1	1600	+39.1	Naraoka *et al.* (2023)
Ryugu A0106 #2	1700	+53.2	Naraoka *et al.* (2023)
Ryugu A0106 #3	1600	+36.7	Naraoka *et al.* (2023)
Ryugu C0107 #2	1300	+39.0	Oba *et al.* (2023)
Ryugu C0107 #3	1400	+32.6	Oba *et al.* (2023)
Ryugu C0107 #4	1500	+38.8	Oba *et al.* (2023)
Ryugu A0105-05*	884.03 ± 24.59	+18.14 ± 0.94	Broadley *et al.* (2023)
Ryugu C0106-06*	855.62 ± 10.34	+19.47 ± 0.89	Broadley *et al.* (2023)
Ryugu A0105-07*	524.44 ± 19.46	+1.7 ± 0.5	Hashizume *et al.* (2024)
Ryugu C0106-07*	616.56 ± 17.36	+0.2 ±0.6	Hashizume *et al.* (2024)

* Pelletised samples analysed by the Hayabusa2-initial-analysis volatile team

Supplementary Information References

Alexander, C.M.O'D., Fogel, M., Yabuta, H., Cody, G.D. (2007) The origin and evolution of chondrites recorded in the elemental and isotopic compositions of their macromolecular organic matter. *Geochimica et Cosmochimica Acta* 71, 4380–4403. https://doi.org/10.1016/j.gca.2007.06.052

Alexander, C.M.O'D., Bowden, R., Fogel, M.L., Howard, K.T., Herd, C.D.K., Nittler, L.R. (2012) The provenances of asteroids, and their contributions to the volatile inventories of the terrestrial planets. *Science* 337, 721–723. https://doi.org/10.1126/science.1223474

Barosch, J., Nittler, L.R., Wang, J., Alexander, C.M.O'D., De Gregorio, B.T. *et al.* (2022) Presolar stardust in asteroid Ryugu. *The Astrophysical Journal Letters* 935, L3. https://doi.org/10.3847/2041-8213/ac83bd

Broadley, M.W., Byrne, D.J., Füri, E., Zimmermann, L., Marty, B. *et al.* (2023) The noble gas and nitrogen relationship between Ryugu and carbonaceous chondrites. *Geochimica et Cosmochimica Acta* 345, 62–74. https://doi.org/10.1016/j.gca.2023.01.020

Chan, Q.H.S., Chikaraishi, Y., Takano, Y., Ogawa, N.O., Ohkouchi, N. (2016) Amino acid compositions in heated carbonaceous chondrites and their compound-specific nitrogen isotopic ratios. *Earth, Planets and Space* 68, 7. https://doi.org/10.1186/s40623-016-0382-8

Grady, M.M., Verchovsky, A.B., Franchi, I.A., Wright, I.P., Pillinger, C.T. (2002) Light element geochemistry of the Tagish Lake CI2 chondrite: Comparison with CI1 and CM2 meteorites. *Meteoritics & Planetary Science* 37, 713–735. https://doi.org/10.1111/j.1945-5100.2002.tb00851.x

Hashizume, K., Marty, B. (2004) Nitrogen isotopic analyses at the sub-picomole level using an ultralow blank laser extraction technique. In: de Groot, P.A. (Ed.) *Handbook of Stable Isotope Analytical Techniques*, *vol. 1*. Elsevier, Amsterdam, 361–374. https://doi.org/10.1016/B978-044451114-0/50019-3

Hashizume, K., Ishida, A., Chiba, A., Okazaki, R., Yogata, K., Yada, T., Kitajima, F., Yurimoto, H., Nakamura, T., Noguchi, T., Yabuta, H., Naraoka, H., Takano, Y., Sakamoto, K., Tachibana, S., Nishimura, M., Nakato, A., Miyazaki, A., Abe, M., Okada, T., Usui, T., Yoshikawa, M., Saiki, T., Terui, F., Tanaka, S., Nakazawa, S., Watanabe, S.-i., Tsuda, Y., Broadley, M.W., Busemann, H. and the Hayabusa2 Initial Analysis Volatile Team. (2024) The Earth atmosphere-like bulk nitrogen isotope composition obtained by stepwise combustion analyses of Ryugu return samples. *Meteoritics & Planetary Science.* https://doi.org/10.1111/maps.14175

Humbert, F., Libourel, G., France-Lanord, C., Zimmermann, L., Marty, B. (2000) CO_2-laser extraction-static mass spectrometry analysis of ultra-low concentrations of nitrogen in silicates. *Geostandards Newsletter* 24, 255-260. https://doi.org/10.1111/j.1751-908X.2000.tb00777.x

Injerd, W.G., Kaplan, I.R. (1974) Nitrogen isotope distribution in meteorites. *Meteoritics* 9, 352.

Kerridge, J.F. (1985) Carbon, hydrogen and nitrogen in carbonaceous chondrites: Abundances and isotopic compositions in bulk samples. *Geochimica et Cosmochimica Acta* 49, 1707–1714. https://doi.org/10.1016/0016-7037(85)90141-3

Matsumoto, T., Noguchi, T., Miyake, A., Igami, Y., Haruta, M. *et al.* (2024) Influx of nitrogen-rich material from the outer Solar System indicated by iron nitride in Ryugu samples. *Nature Astronomy* 8, 207–215. https://doi.org/10.1038/s41550-023-02137-z

Nakamura, E., Kobayashi, K., Tanaka, R., Kunihiro, T., Kitagawa, H. *et al.* (2022) On the origin and evolution of the asteroid Ryugu: A comprehensive geochemical perspective. *Proceedings of the Japan Academy, Series B* 98, 227–282. https://doi.org/10.2183/pjab.98.015

Naraoka, H., Takano, Y., Dworkin, J.P., Oba, Y., Hamase, K. *et al.* (2023) Soluble organic molecules in samples of the carbonaceous asteroid (162173) Ryugu. *Science* 379, eabn9033. https://doi.org/10.1126/science.abn9033

Nguyen, A.N., Mane, P., Keller, L.P., Piani, L., Abe, Y. *et al.* (2023) Abundant presolar grains and primordial organics preserved in carbon-rich exogenous clasts in asteroid Ryugu. *Science Advances* 9, eadh1003. https://doi.org/10.1126/sciadv.adh1003

Nier, A.O. (1950) A redetermination of the relative abundances of the isotopes of carbon, nitrogen, oxygen, argon, and potassium. *Physical Review* 77, 789–793. https://doi.org/10.1103/PhysRev.77.789

Oba, Y., Koga, T., Takano, Y., Ogawa, N.O., Ohkouchi, N. *et al.* (2023) Uracil in the carbonaceous asteroid (162173) Ryugu. *Nature Communications* 14, 1292. https://doi.org/10.1038/s41467-023-36904-3

Pearson, V.K., Sephton, M.A., Franchi, I.A., Gibson, J.M., Gilmour, I. (2006) Carbon and nitrogen in carbonaceous chondrites: Elemental abundances and stable isotopic compositions. *Meteoritics & Planetary Science* 41, 1899–1918. https://doi.org/10.1111/j.1945-5100.2006.tb00459.x

Pilorget, C., Okada, T., Hamm, V., Brunetto, R., Yada, T. *et al.* (2022) First compositional analysis of Ryugu samples by the MicrOmega hyperspectral microscope. *Nature Astronomy* 6, 221–225. https://doi.org/10.1038/s41550-021-01549-z

Quirico, E., Bonal, L., Beck, P., Alexander, C.M.O'D., Yabuta, H., Nakamura, T., Nakato, A., Flandinet, L., Montagnac, G., Schmitt-Kopplin, P., Herd, C.D.K. (2018) Prevalence and nature of heating processes in CM and C2-ungrouped chondrites as revealed by insoluble organic matter. *Geochimica et Cosmochimica Acta* 241, 17–37. https://doi.org/10.1016/j.gca.2018.08.029

Robert, F., Epstein S. (1982) The concentration and isotopic composition of hydrogen, carbon and nitrogen in carbonaceous meteorites. *Geochimica et Cosmochimica Acta* 46, 81–89. https://doi.org/10.1016/0016-7037(82)90293-9

Robinson, B.W., Kusakabe, M. (1975) Quantitative preparation of sulfur dioxide, for $^{34}S/^{32}S$ analyses, from sulfides by combustion with cuprous oxide. *Analytical Chemistry* 47, 1179–1181. https://doi.org/10.1021/ac60357a026

Russell, S.S., Arden, J.W., Pillinger, C.T. (1996) A carbon and nitrogen isotope study of diamond from primitive chondrites. *Meteoritics & Planetary Science* 31, 343–355. https://doi.org/10.1111/j.1945-5100.1996.tb02071.x

Sephton, M.A., Verchovsky, A.B., Bland, P.A., Gilmour, I., Grady, M.M., Wright, I.P. (2003) Investigating the variations in carbon and nitrogen isotopes in carbonaceous chondrites. *Geochimica et Cosmochimica Acta* 67, 2093–2108. https://doi.org/10.1016/S0016-7037(02)01320-0

Verchovsky, A.B. (2017) Origin of isotopically light nitrogen in meteorites. *Geochemistry International* 55, 957–970. https://doi.org/10.1134/S0016702917110106

Yabuta, H., Cody, G.D., Engrand, C., Kebukawa, Y., De Gregorio, B. *et al.* (2023) Macromolecular organic matter in samples of the asteroid (162173) Ryugu. *Science* 379, eabn9057. https://doi.org/10.1126/science.abn9057

Zimmermann, L., Burnard, P., Marty, B., Gaboriaud, F. (2009) Laser Ablation (193 nm), Purification and Determination of Very Low Concentrations of Solar Wind Nitrogen Implanted in Targets from the GENESIS Spacecraft. *Geostandards and Geoanalytical Research* 33, 183–194. https://doi.org/10.1111/j.1751-908X.2009.00021.x

Zimmermann, L., Bekaert, D. (2020) Analyse des gaz rares par spectrométrie de masse statique - Mesures et applications. Techniques de l'ingénieur J6637 v1. https://doi.org/10.51257/a-v1-j6637